Radiology

White Matter Degeneration with Aging: Longitudinal Diffusion MR Imaging Analysis[1]

Marius de Groot, PhD
Lotte G. M. Cremers, MD
M. Arfan Ikram, MD, PhD
Albert Hofman, MD, PhD
Gabriel P. Krestin, MD, PhD
Aad van der Lugt, MD, PhD
Wiro J. Niessen PhD
Meike W. Vernooij, MD, PhD

Purpose: To determine longitudinally the rate of change in diffusion-tensor imaging (DTI) parameters of white matter microstructure with aging and to investigate whether cardiovascular risk factors influence this longitudinal change.

Materials and Methods: This prospective population-based cohort study was approved by a dedicated ethics committee overseen by the national government, and all participants gave written informed consent. Community-dwelling participants without dementia were examined by using a research-dedicated 1.5-T magnetic resonance (MR) imager on two separate visits that were, on average, 2.0 years apart. Among 810 persons who were eligible for imaging at baseline, longitudinal imaging data were available for 501 persons (mean age, 69.9 years; age range, 64.1–91.1 years). Changes in normal-appearing white matter DTI characteristics in the tract centers were analyzed globally to investigate diffuse patterns of change and then locally by using voxelwise multilinear regression. The influence of cardiovascular risk factors was assessed by treating them as additional determinants in both analyses.

Results: Over the 2.0-year follow-up interval, global fractional anisotropy (FA) decreased by 0.0042 ($P < .001$), while mean diffusivity (MD) increased by 8.1×10^{-6} mm^2/sec ($P < .001$). Voxelwise analysis of the brain white matter skeleton showed an average decrease of 0.0082 (P_{mean} = .002) in FA in 57% of skeleton voxels. The sensorimotor pathway, however, showed an increase of 0.0078 (P_{mean} = .009) in FA. MD increased by 10.8×10^{-6}mm^2/sec ($P_{mean} < .001$) on average in 79% of white matter skeleton voxels. Additionally, white matter degeneration was more pronounced in older persons. Cardiovascular risk factors were generally not associated with longitudinal changes in white matter microstructure.

Conclusion: Longitudinal diffusion analysis indicates widespread microstructural deterioration of the normal-appearing white matter in normal aging, with relative sparing of sensorimotor fibers.

Online supplemental material is available for this article.

[1] From the Departments of Radiology (M.d.G., L.G.M.C., M.A.I., G.P.K., A.v.d.L., W.J.N., M.W.V.), Medical Informatics (M.d.G., W.J.N.), Epidemiology (M.d.G., L.G.M.C., M.A.I., A.H., M.W.V.), and Neurology (M.A.I.), Erasmus MC, University Medical Center Rotterdam, PO Box 2040, Room Ca220, 3000 CA Rotterdam, the Netherlands; and Department of Imaging Science and Technology, Faculty of Applied Sciences, Delft University of Technology, Delft, the Netherlands (W.J.N.). Received January 26, 2015; revision requested March 26; revision received July 15; accepted July 31; final version accepted August 27. Supported by Erasmus MC MRACE grant 2011, the Internationale Stichting Alzheimer Onderzoek (ISAO) grant number #12533, ZonMW Veni-grant 916.13.054, European Union's Seventh Framework Programme: project VPH-Dare@IT (FP7-ICT-2011-9-601055), and the STW Perspectief programme Population Imaging Genetics (ImaGene) projects 12722 and 12723 supported by the Dutch Technology Foundation STW, which is part of the Netherlands Organisation for Scientific Research (NWO) and is partly funded by the Dutch Ministry of Economic Affairs. **Address correspondence to** M.W.V. (e-mail: *m.vernooij@erasmusmc.nl*).

It has been recognized that both gray matter loss and white matter deterioration play an important role in brain aging and cognitive decline (1), and a vascular etiologic pathway has often been hypothesized (2). Diffusion-tensor imaging (DTI) is a noninvasive magnetic resonance (MR) imaging technique that enables measurement of diffusion of water and can be used to quantify subtle changes of white matter tissue organization that are not visible at structural MR imaging. DTI provides multiple descriptors of diffusion, with fractional anisotropy (FA) and mean diffusivity (MD) most widely used. FA describes the directionality of diffusion, and a lower value typically reflects reduced microstructural organization in regions where white matter fibers are aligned. MD represents the overall magnitude of water diffusion, and a higher value generally reflects reduced microstructural organization (3).

Reduced microstructural white matter organization possibly impedes communication within and between neurocognitive networks, which might result in cognitive impairment (4). To identify persons at higher risk of neurodegenerative disease, it is important to quantify changes in brain tissue at an early stage (5). This, however, also requires characterization of baseline age-related changes.

The quantitative nature makes DTI very suitable for longitudinal analyses, which are likely to be more sensitive in the early detection of changes in white matter microstructure. However, longitudinal data are still scarce, and studies are mostly performed with small sample sizes and in patients with cognitive impairment or Alzheimer disease (6–9). The sparse longitudinal findings in persons experiencing normal aging did, however, corroborate evidence from cross-sectional studies that showed that during normal aging, white matter shows lower FA, with less-uniform observations for regions with crossing fibers, combined with higher MD (6–11), and that those aging effects differ across brain regions (8,9,12,13). However, these results need to be corroborated in larger longitudinal studies.

Thus, in the current study, we aimed to longitudinally determine the rate of change in DTI parameters of white matter microstructure in aging and to investigate whether cardiovascular risk factors influence this longitudinal change (14,15).

Advances in Knowledge

- The microstructure of brain white matter diffusely deteriorates with aging (global fractional anisotropy [FA] decreases by 0.0042 [$P < .001$], while mean diffusivity [MD] increases by 8.1 $\times 10^{-6}$mm^2/sec [$P < .001$] over a 2.0-year follow-up).
- Voxelwise changes in white matter microstructure occur in 57% (decrease in FA) and 79% (increase in MD) of white matter tract centers (average FA decrease, 0.0082 [$P_{mean} = .002$]; average MD increase, 10.8 $\times 10^{-6}$mm^2/sec [$P_{mean} < .001$] over the 2.0-year follow-up).
- Sensorimotor fibers appear to be relatively preserved in patients with age-related degeneration; in those voxels that exhibit paradoxical FA increase, FA increases on average by 0.0078 ($P_{mean} = .009$), despite increase in MD in most of this region (average increase of 10.2 $\times 10^{-6}$mm^2/sec [$P_{mean} < .001$]).
- White matter deterioration appears more prominent in older persons, indicating a nonlinear trajectory of age-related deterioration; within centers of white matter tracts, 44% of the voxels showed additional changes associated with higher age (P_{mean} for FA, .03; P_{mean} for MD, .02).

Materials and Methods

Study Population

This study is based on participants from the Rotterdam Study, a prospective population-based cohort study that investigates causes and consequences of age-related diseases (16). The original study population consisted of 7983 participants aged 55 years or older within Ommoord, a suburb of Rotterdam, the Netherlands. In 2000, the cohort was expanded by an additional 3011 persons aged 55 years or older who were living in the study area and were not included before (16). Since 2005, brain MR imaging has been incorporated in the core protocol of the study. In 2005 and 2006, a group of 1073 participants was randomly selected from the cohort expansion to participate in the Rotterdam Scan Study (17). Participants underwent imaging three times: once in 2005 or 2006, once in 2008 or 2009, and once in 2011 or 2012. The latter two imaging examinations included an upgraded DTI acquisition that was used in the current analysis, defining the 2008 or 2009 examination as the baseline study and the 2011 or 2012 examination as the follow-up study. We excluded individuals who, at either time point, had dementia or who had MR imaging contraindications, including claustrophobia. For the 2008 or 2009 examination, 899 of the original 1073 persons could be invited, of whom 810 were eligible and 741 participated. At follow-up in 2011 or 2012, 649 of 741

Published online before print
10.1148/radiol.2015150103 **Content code:** NR

Radiology 2016; 279:532–541

Abbreviations:
DTI = diffusion-tensor imaging
FA = fractional anisotropy
ICV = intracranial volume
MD = mean diffusivity
TBSS = tract-based spatial statistics
WML = white matter lesion

Author contributions:
Guarantors of integrity of entire study, M.d.G., M.W.V.; study concepts/study design or data acquisition or data analysis/interpretation, all authors; manuscript drafting or manuscript revision for important intellectual content, all authors; approval of final version of submitted manuscript, all authors; agrees to ensure any questions related to the work are appropriately resolved, all authors; literature research, M.d.G., L.G.M.C., M.W.V.; clinical studies, M.A.I., A.v.d.L.; statistical analysis, M.d.G., L.G.M.C., M.A.I.; and manuscript editing, all authors

Conflicts of interest are listed at the end of this article.

participants were reinvited; of these, 625 were eligible and 548 participated. We excluded participants with incomplete image acquisition (n = 5), those with MR imaging–defined cortical infarcts (n = 20), and those with imaging artifacts that hampered automated processing (n = 22); thus, we were left with 501 participants with longitudinal DTI data available for analysis. A flowchart for participant inclusion is shown in Figure 1. The Rotterdam Study has been approved by the medical ethics committee according to the Population Study Act Rotterdam Study, executed by the Ministry of Health, Welfare and Sports of the Netherlands. Written informed consent was obtained from all participants.

Figure 1

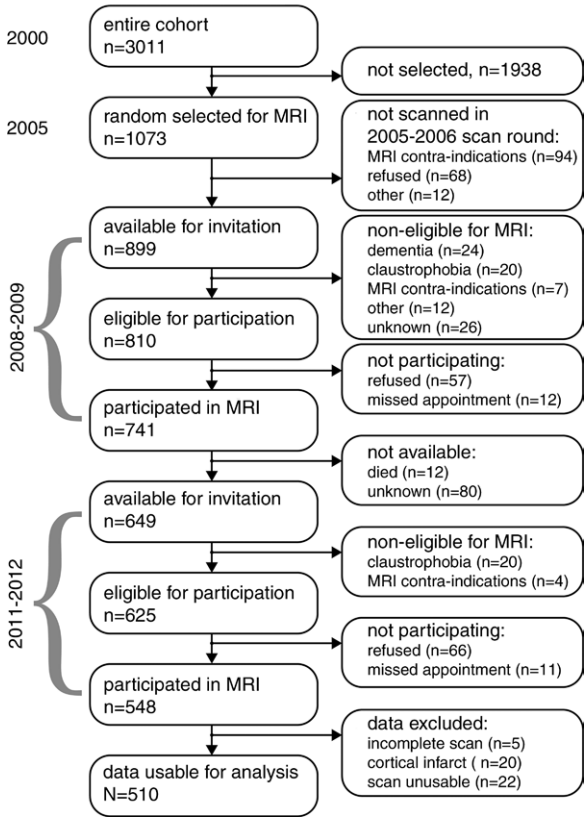

Figure 1: Flowchart shows inclusion and exclusion of study participants.

MR Imaging

Multisequence MR imaging was performed with identical imaging parameters at both time points with a 1.5-T imager (Signa Excite; GE Healthcare, Milwaukee, Wis) dedicated to the study and maintained without major hardware or software updates (17). In short, imaging included a T1-weighted three-dimensional fast radiofrequency spoiled gradient-recalled acquisition in the steady state with an inversion recovery prepulse sequence, a proton density–weighted sequence, and a T2-weighted fluid-attenuated inversion recovery sequence (17). For DTI, we performed a single-shot diffusion-weighted spin-echo echo-planar imaging sequence (repetition time msec/echo time msec, 8575/82.6; field of view, 210 × 210 mm; matrix, 96 × 64 [zero-padded in k-space to 256 × 256] section thickness, 3.5 mm; 35 contiguous sections). Maximum b value was 1000 sec/mm^2 in 25 noncollinear directions; three b_0 volumes were acquired without diffusion weighting (b value, 0 sec/mm^2).

Tissue Segmentation

Baseline examinations were segmented into gray matter, white matter, cerebrospinal fluid, and background tissue by using an automatic segmentation method (18). An automatic postprocessing step distinguished normal-appearing white matter from white matter lesions (WMLs) based on the fluid-attenuated inversion recovery image and the tissue segmentation (19). Intracranial volume (ICV) (excluding the cerebellum with surrounding cerebrospinal fluid) was estimated by summing total gray matter, white matter, and cerebrospinal fluid volumes. The WML segmentation was mapped into DTI image space by using boundary-based registration (20) performed on the white matter segmentation, the b_0, and T1-weighted images.

DTI Processing

Diffusion data were preprocessed with a standardized processing pipeline (21). In short, DTI data were corrected for subject motion and eddy currents by affine coregistration of the diffusion-weighted volumes to the b_0 volumes, including correction of gradient vector directions. Diffusion tensors were estimated by using a nonlinear Levenberg-Marquardt estimator, available in ExploreDTI (22). FA and MD, measures of tissue microstructure, were computed from the diffusion tensor images. Tensor fits were inspected for artifacts by reviewing axial sections of the FA images (M.d.G., a researcher with 5 years of experience in diffusion image analysis; L.G.M.C., a radiologist-in-training with 2 years of experience in diffusion image analysis).

Image Registration

Intrasubject correspondence (between the two time points) and intersubject correspondence were achieved by means of image registration. Improved tract-based spatial statistics (TBSS) were used with optimized high degrees of freedom registration in lieu of the two-stage registration-projection approach implemented as part of the

original TBSS method (23,24). This registration approach is described in Appendix E1 (online). All registrations were inspected by reviewing axial compilations of superpositioned moving and target images (M.d.G., L.G.M.C.). After registration, individual change in diffusion measures could be computed in standard space (Montreal Neurological Institute 152 template, as provided with the FSL software [25]) by subtracting baseline images from follow-up images.

A study-specific white matter skeleton was constructed by using the TBSS skeletonization procedure on the average FA image composed of all subject images at both time points combined in standard space, thresholding the FA skeleton at 0.25. This skeleton was then used to mask the difference images for longitudinal statistical analysis.

Assessment of Risk Factors

The following cardiovascular risk factors were assessed based on information derived from home interviews and physical examinations (16) at one time point prior to baseline MR imaging. Blood pressure was measured twice with the participant seated by using a random-zero sphygmomanometer. Use of antihypertensive drugs was recorded. Diabetes mellitus status was determined based on fasting serum glucose level (≥7.0 mmol/L), nonfasting serum glucose level (≥11.1 mmol/L), or use of antidiabetic medication. Smoking history was assessed by interview, and participants were classified as those who had never smoked, former smokers, or current smokers. Total and high-density lipoprotein cholesterol levels were determined in blood serum, while recording the use of lipid-lowering medication. Apolipoprotein E *(APOE)* ε4 allele carriership was assessed with coded genomic DNA samples. Assessment of risk factors predated baseline MR imaging by 3 years, on average.

Statistical Analysis

Changes in diffusion characteristics were assessed both globally and locally by using skeletonized difference measurements. For global analysis, we investigated the average change in FA and MD over the entire skeleton per subject, excluding voxels labeled as WML at baseline examination. We assessed whether there was a global change in diffusion measurements with multiple linear regression by using three models. In model 1, we adjusted for age, sex, imaging interval, and ICV. In addition, we considered alternatives to model 1, in which we corrected for individual measures of the white matter macrostructure: white matter atrophy (using normal-appearing white matter volume) or WML load (natural log-transformed to correct for the skewed volume distribution) instead of age. In model 2, we additionally adjusted for both white matter atrophy and WML load to identify changes in white matter microstructure independent from macrostructural white matter changes that may also affect diffusivity measurements. In model 3, we added the different cardiovascular risk factors individually to model 1 to separately investigate the effect of these on change in white matter microstructure. For analyses with blood pressure and cholesterol, medication use was considered a confounder and was added to the model. For analysis of total cholesterol level, high-density lipoprotein cholesterol level was additionally included as a confounder. All global analyses were performed by using SPSS statistical software (version 20; IBM, Armonk, NY).

For the localized TBSS analyses, we performed voxelwise multiple linear regression analysis for the same models as the global analyses, also restricting the analyses to the (baseline) normal-appearing white matter. If significant associations were found for tests in model 3, we additionally performed an analysis correcting for measures of macrostructural white matter degeneration to rule out confounding by white matter atrophy and WML. We used threshold-free cluster enhancement (26) with default settings for skeletonized data to promote spatially clustered findings and controlled the family-wise error rate by using a permutation-based approach (using 5000 permutations) (27). All analyses were performed by using an in-house–adapted version of the Randomise tool available in FSL software (25), which discarded WML voxels in every permutation, effectively performing a voxelwise available-case analysis.

Results

Table 1 shows the population characteristics of the 501 participants. Mean age at baseline MR imaging was 69.9 years (range, 64.1–91.1 years), and 253 (50.5%) participants were

Table 1

Population Characteristics

Characteristic	Finding
Age (y)	69.9 ± 4.3
Female sex	253 (50.5)
Follow-up time (y)	2.0 ± 0.5
NAWM baseline FA	0.322 ± 0.016
NAWM baseline MD ($\times 10^{-3}$mm^2/sec)	0.726 ± 0.022
Brain volume (mL)	1125 ± 114
NAWM volume (mL)	394 ± 58
WML volume (mL)*	3.74 (2.28–7.39)
Systolic blood pressure (mmHg)	142.3 ± 16.5
Diastolic blood pressure (mmHg)	80.9 ± 9.7
Use of blood pressure–lowering medication	168 (33.7)
Diabetes mellitus	34 (6.9)
Smoking history	
Never	162 (32.7)
Former	270 (54.4)
Current	64 (12.9)
Total serum cholesterol level (mmol/L)	5.73 ± 0.94
Serum high-density lipoprotein cholesterol level (mmol/L)	1.45 ± 0.40
Use of lipid-lowering medication	107 (21.4)
APOE ε4 carriership	118 (24.3)

Note.—Unless otherwise indicated, data are either mean ± standard deviation or number of patients with the percentage in parentheses. A total of 501 persons were included; however, the following variables had missing data: blood pressure (n = 4), use of blood pressure–lowering medication (n = 2, overlapping with blood pressure), diabetes mellitus (n = 5), smoking history (n = 5), total serum cholesterol level (n = 3), use of lipid-lowering medication (n = 2, not overlapping with cholesterol), and *APOE* ε4 carriership (n = 15). NAWM = normal-appearing white matter.

* Data are median, and data in parentheses are interquartile range.

female. The global analyses, corrected for age, sex, imaging interval, and ICV, showed an average decrease of 0.0042 ($P < .001$) for FA in the normal-appearing white matter skeleton and an average increase of 8.1 × 10^{-6} mm^2/sec ($P < .001$) for MD over the follow-up interval (model 1). The same changes were observed when we additionally controlled for white matter atrophy and WML load (model 2). As shown in Table 2, these two additional confounding variables also were associated with changes in MD (ie, higher WML load, less normal-appearing white matter, and higher age resulted in an additional increase in MD) but were not associated with changes in FA.

Voxelwise analyses, seen in Figure 2 for model 2, revealed a decrease in FA of, on average, 0.0082 ($P_{mean} = .002$) in 57% of the white matter skeleton over the follow-up interval. However, in most of the sensorimotor tracts, FA paradoxically increased by 0.0078 ($P_{mean} = .009$), on average. Change over time for models 1 and 2 was not materially different. Increase in FA was found in the sensorimotor tracts extending from the brain stem through the internal capsule (both the anterior limb and the posterior limb) and the corona radiata up into the motor cortex (Fig 2) and amounted to 8.5% of the white matter skeleton. MD increased throughout the brain by, on average, 10.8 × 10^{-6} mm^2/sec ($P_{mean} < .001$) in 79% of the white matter skeleton. The most marked increase was found periventricularly and around the fornix. No voxels showed a significant decrease in MD. Among the voxels that expressed increased FA, MD mostly increased by 10.2 × 10^{-6} mm^2/sec ($P_{mean} < .001$), on average. By constraining the voxelwise analysis to the normal-appearing white matter, the number of degrees of freedom of the analysis varied from voxel to voxel; however, variation was smooth, and the minimum number of subjects included per voxel for models 1 and 2 was 295.

Figures 3 and 4 show how changes in FA (Fig 3) and MD (Fig 4) depended on various parameters included in models 1 and 2. For model 1, we observed associations between age and FA (decrease) or MD (increase) in 44% of the skeleton voxels (for FA, $P_{mean} = .03$; for MD, $P_{mean} = .02$). These associations were reduced both in strength and in extent (changes in

Table 2

Demographic Characteristics and Global Change in White Matter Microstructure

Variable	Change in FA (× 10^{-3})	*P* Value	Change in MD (× $10^{-6}$$mm^2$/sec)	*P* Value
Age	−0.12	.09	0.20*	.01
Sex	0.37	.57	−0.07	.93
Brain volume	−0.18	.69	0.91	.08
Normal-appearing white matter volume	0.27	.51	−1.43*	.002
ln (WML volume)	−0.29	.31	1.21*	<.001

* Data are significantly different.

Figure 2

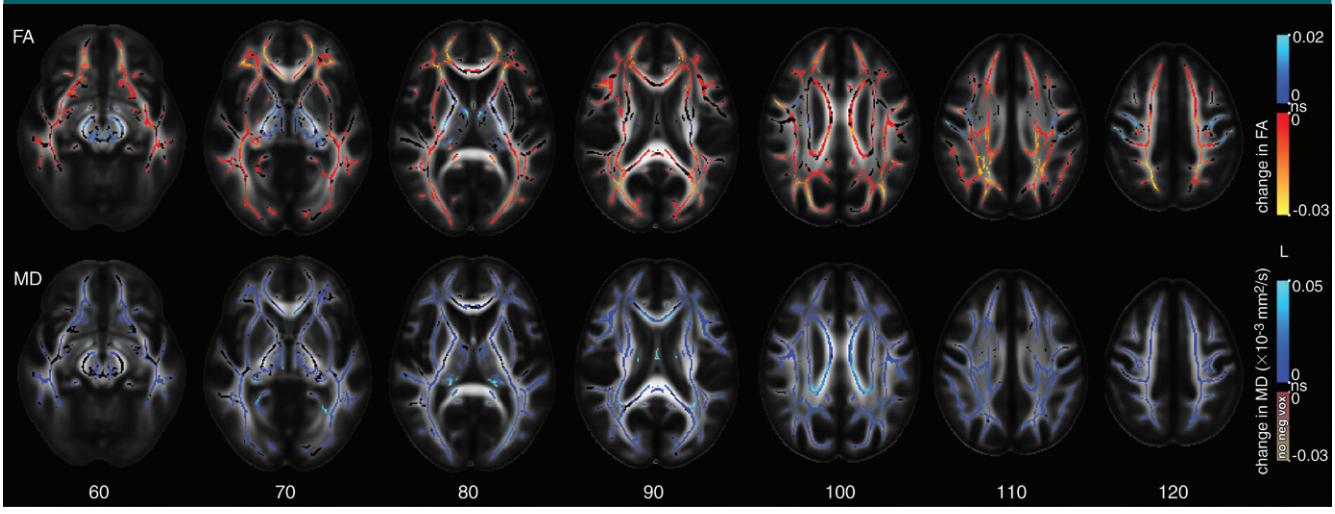

Figure 2: Change in diffusion characteristics over 2 years of follow-up, corrected for age, sex, imaging interval, intracranial volume, and macroscopic white matter changes. Top row: Regions of significant ($P < .05$) change in FA over time. Blue indicates an increase in FA; red and yellow indicate a decrease in FA. Bottom row: Regions of significant ($P < .05$) change in mean diffusivity MD. Blue indicates an increase in MD. No voxels showed a significant decrease in MD. The familywise error rate was controlled using a permutation approach. *P* values are presented in Figure E2 (online). Results are overlaid on a population-specific average FA image in standard space coordinates, showing nonsignificant (ns) skeleton voxels in black.

Figure 3

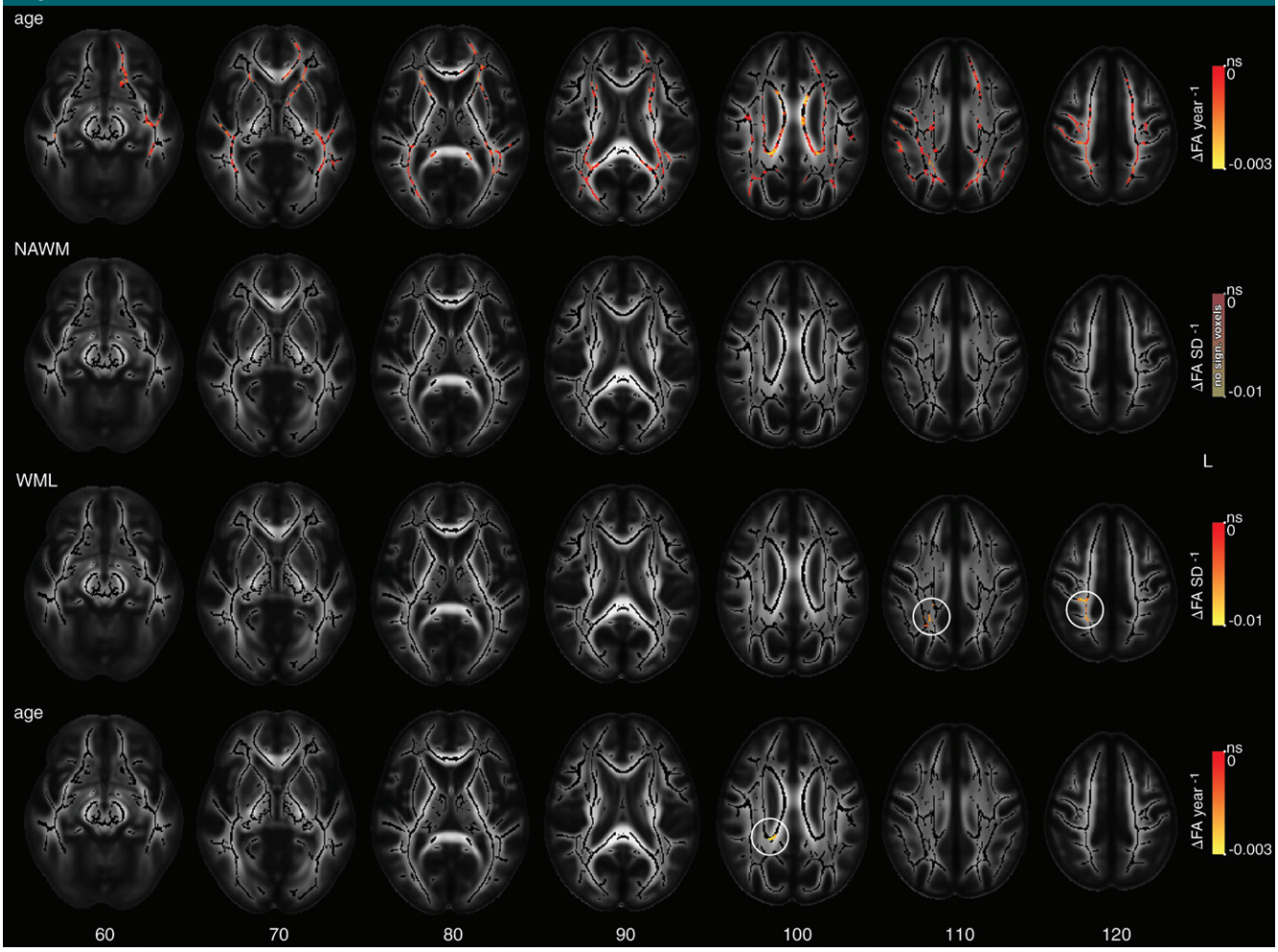

Figure 3: Age and macrostructural white matter changes at baseline and change in FA over 2 years of follow-up. Top row: In yellow to red regions, there is a decrease in FA that relates to higher age at baseline (adjusted for sex, imaging interval, and ICV). Middle rows: FA changes that are associated with a decrease in normal-appearing white matter *(NAWM)* volume and an increase in WML volume. (Both were adjusted for age, sex, imaging interval, and ICV). Bottom row: Regions of decrease in FA related to older age, when additionally adjusted for normal-appearing white matter volume and WML volume. Inverse directions of association showed no significant voxels (not shown). Results shown are significant ($P < .05$); the family-wise error rate was controlled by using a permutation approach. *P* values are shown in Figure E3 (online). Results are overlaid on a population-specific average FA image in standard space coordinates and show nonsignificant normal-appearing white matter skeleton voxels in black.

9.4% of skeleton voxels) when we added measures of macrostructural white matter changes (white matter atrophy and WML load) in the model. The figures also show associations between white matter atrophy and WML load and change in FA and MD in model 2. Figure E1a (online) shows the separate associations for white matter atrophy and WML load not corrected for age (alternatives to model 1). No difference in change in diffusion characteristics was observed for men or women. Graphs showing *P* values for the analyses are shown in Figures E1–E4 (online).

When investigating cardiovascular risk factors in relation to longitudinal DTI changes, we found associations for only *APOE* ε4 carriership and total serum cholesterol level. Specifically, ε4 carriers showed localized increases in FA in comparison to noncarriers, but there were no changes globally. These local differences were more prominent in the right hemisphere than in the left hemisphere and occurred primarily in the centrum semiovale and in the white matter adjacent to the trigone of the lateral ventricle. In contrast, we observed lower MD only in a small peritrigonal cluster in carriers compared with noncarriers. These observed associations persisted when we additionally corrected for macrostructural measures of white matter

Figure 4

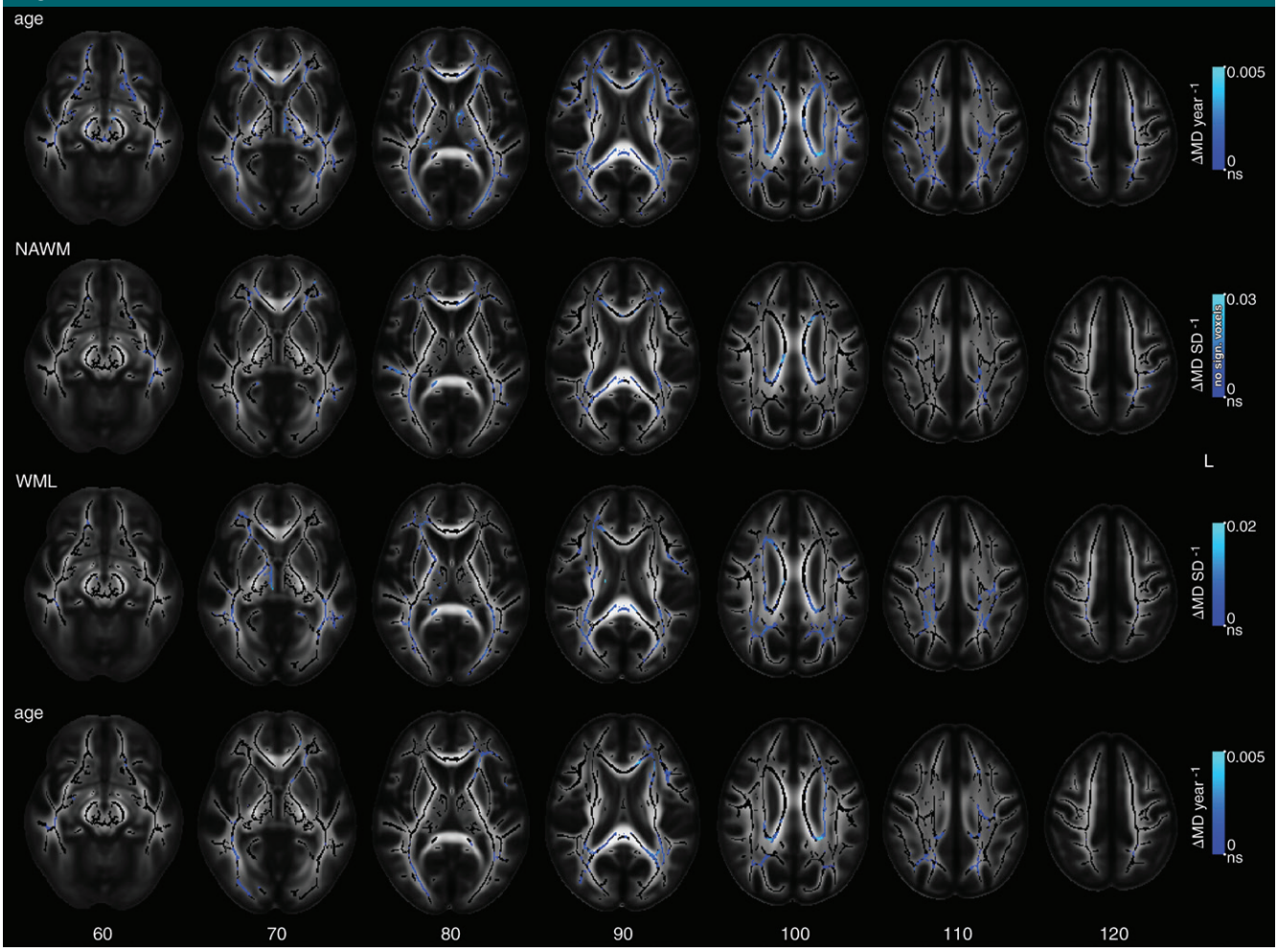

Figure 4: Age and macrostructural white matter changes at baseline and change in MD over 2 years of follow-up. Top row: Blue regions show an increase in MD that relates to higher age at baseline (adjusted for sex, imaging interval, and ICV). Middle rows: MD changes are associated with a decrease in normal-appearing white matter *(NAWM)* volume and an increase in WML volume. (Both were adjusted for age, sex, imaging interval, and ICV). Bottom row: Regions of increase in MD related to older age, when adjusted for normal-appearing white matter volume and WML volume. Inverse directions of association showed no significant voxels (not shown). Results shown are significant ($P < .05$). The family-wise error rate was controlled by using a permutation approach. *P* values are presented in Figure E4 (online). Results are overlaid on a population-specific average FA image in standard space coordinates and show nonsignificant normal-appearing white matter skeleton voxels in black.

degeneration. Similarly, we observed that *APOE* ε4 carriers had a smaller global increase in MD (Table 3).

Total serum cholesterol level was associated locally with a greater increase in MD in the left hemisphere. Regions included the corona radiata and white matter around the posterior and anterior horns of the lateral ventricle. These observed associations persisted when additionally correcting for macrostructural measures of white matter degeneration. Other cardiovascular risk factors were associated with neither global nor local changes in tissue microstructure. Results for global DTI characteristics are presented in Table 3.

Discussion

In this large population-based longitudinal sample of elderly persons, we found changes to microstructural tissue organization congruent with microstructural white matter deterioration. Over a 2-year follow-up interval, loss of microstructure was globally reflected in decreases in FA and increases in MD, independent of severity of white matter atrophy and WML load. On a voxelwise level, we found regional differences in white matter changes, with decreased FA in most of the brain but increased FA in most of the sensorimotor pathway running from the brain stem up to the motor cortex. In contrast, MD was increased throughout the white matter skeleton, without any

Table 3

Cardiovascular Risk Factors and Global Change in White Matter Microstructure

Risk or Protective Factor	Change in FA ($\times 10^{-3}$)	*P* Value	Change in MD ($\times 10^{-6}$mm^2/sec)	*P* Value
Systolic blood pressure	−0.46	.09	0.33	.29
Diastolic blood pressure	−0.01	.98	0.10	.76
Diabetes mellitus	0.08	.77	0.46	.13
Smoking (never-current)	−0.15	.86	0.22	.83
Total serum cholesterol level	−0.42	.15	−0.09	.78
Serum high-density lipoprotein cholesterol level	0.31	.28	−0.23	.49
APOE ε4 carriership	1.12	.07	−1.51*	.04

Note.—Data represent change in diffusion measure, per standard deviation of change for continuous variables or absolute for categorical variables.

* Data are significantly different.

significant decreases. We found that white matter deterioration was locally more pronounced with higher age, indicating that older persons show more change in white matter microstructure over the same follow-up time than do younger persons. This could partly be explained by macroscopic measures of white matter degeneration (ie, white matter atrophy and WML load), which also increase with age. We identified only a few associations between known (cardiovascular) determinants of white matter atrophy and WML load and changes in diffusion characteristics over time, both globally and locally. These findings contribute to our understanding of age-related brain changes and may aid in the future identification of early abnormalities leading to disease.

Cross-sectional studies of normal aging of white matter generally have shown lower FA and higher MD with higher age (1,11,12), which is in line with our results. In a cross-sectional analysis of an earlier time point in the same population, we found a similar effect with age itself (ie, most of the associations with age were driven by macroscopic measures of white matter degeneration) (10). Both results indicate that white matter degeneration with aging is not intrinsically due to aging alone, nor is it purely driven by macroscopic measures of white matter degeneration. Longitudinal analyses, which are necessary to reliably characterize change over time, have revealed reductions in FA and increases in MD (6,9). Our findings enable us to confirm many of these longitudinal and cross-sectional findings and to extend on these for the normal-appearing white matter in a larger population.

In the sensorimotor pathway, we identified a seemingly paradoxical increase of FA, which may have been related to partial volume mixing of multiple fiber tracts (eg, crossing or touching fibers) within these voxels. Selective degeneration of one fiber bundle with relative sparing of the other bundle may lead to an increase in FA, with a concomitant increase in MD. This effect was previously observed in a study on Wallerian degeneration (28) and was described in detail in a cross-sectional study on Alzheimer disease (29). The increased FA, ascending from the brain stem through the internal capsule and the corona radiata up into the motor cortex (ie, regions with either crossing fibers or closely spaced adjacent fibers [30,31]) seems to indicate a relative sparing of sensorimotor fibers. Inside the fornix, we found the strongest increase in MD. This may reflect loss of microstructural organization in this limbic fiber, but we should note that this tract is small compared with our imaging matrix and is surrounded by cerebrospinal fluid. Thus, these findings likely represent a combination of micro- and macrostructural (ie, tract thinning) changes (32).

We did observe counterintuitive associations with *APOE* ε4 carriership. Globally, we observed a decrease in MD in *APOE* ε4 carriers compared with that in noncarriers. Locally, we observed increases in FA in *APOE* ε4 carriers in comparison with FA in noncarriers in regions with a high prevalence of WML. These observations are in contrast to the findings of cross-sectional studies with *APOE* genotype that have generally shown widespread deterioration of white matter microstructure associated with the ε4 allele (33,34). On closer inspection, this paradoxical increase in FA was largely explained by lower baseline FA in carriers and a larger decrease in FA in noncarriers. Higher serum cholesterol level was associated with stronger increases in MD over time in the left hemisphere. When we investigated other cardiovascular risk factors, we observed associations with neither global nor local changes to white matter microstructure; this finding was in line with the findings of another longitudinal study (6) but was in disagreement with cross-sectional observations (2,35). These discrepancies, both for *APOE* and for cardiovascular factors, might have been due to the relatively short follow-up interval, which translates in the (clustered) voxelwise and global statistics being relatively underpowered. Another possibility is that changes induced by cardiovascular risk factors may be more prominent in the periphery of white matter tracts, whereas the TBSS method focused on tract centers. Most importantly however, our longitudinal design only probes differential effects and not the difference accumulated over the total exposure time, which precludes the analysis from finding subtle differential changes with cardiovascular risk factors.

Our study had several limitations. First, the relatively short follow-up interval may have limited sensitivity to detect differences over time, especially in the case of differential effects with risk factors (as mentioned previously). This meant we could not disambiguate

the risk factor–related changes from the large changes associated with aging. This also impeded direct translation of our findings to individual subjects (eg, for use in clinical care). Second, the study protocol was defined in 2005 and 2006; therefore, the spatial resolution for the diffusion acquisition was relatively poor for current standards (23). Although use of TBSS mitigated partial volume effects in the major white matter tracts and although we adjusted for overall white matter atrophy, the resolution reduced sensitivity to detect change in very thin tracts. Nevertheless, we identified widespread deterioration of white matter microstructure within the studied interval. Third, we excluded participants with dementia at either time point, but we did not exclude persons with mild cognitive impairment, since mild cognitive impairment contributes to the continuous spectrum of age-related diseases that we aimed to investigate. This may have led to inclusion of some persons with preclinical dementia, which could have affected our results.

In conclusion, in this large longitudinal analysis of brain white matter microstructure in normal aging, we found widespread microstructural deterioration of the normal-appearing white matter, with relative sparing of sensorimotor fibers. We found changes to be more prominent in older persons. This finding was partly explained by concomitant macroscopic white matter damage. Cardiovascular risk factors did not generally relate to white matter microstructure. These insights into white matter degeneration in aging may help us to understand the pathophysiology of neurodegenerative diseases.

Disclosures of Conflicts of Interest: M.d.G. disclosed no relevant relationships. **L.G.M.C.** disclosed no relevant relationships. **M.A.I.** disclosed no relevant relationships. **A.H.** disclosed no relevant relationships. **G.P.K.** Activities related to the present article: disclosed no relevant relationships. Activities not related to the present article: is a consultant to Bracco; received grants from Siemens, Bayer, GE Healthcare, and Bracco. Other relationships: disclosed no relevant relationships. **A.v.d.L.** disclosed no relevant relationships. **W.J.N.** Activities related to the present article: disclosed no relevant relationships. Activities not related to the present article: cofounder and shareholder of Quantib, has a patent pending (PCT/NL2015/050505, Detection of asymmetry in percentile value for QIB, VO reference P107431PC00). Other relationships: disclosed no relevant relationships. **M.W.V.** disclosed no relevant relationships.

References

1. Sullivan EV, Pfefferbaum A. Diffusion tensor imaging and aging. Neurosci Biobehav Rev 2006;30(6):749–761.
2. Gons RA, van Oudheusden LJ, de Laat KF, et al. Hypertension is related to the microstructure of the corpus callosum: the RUN DMC study. J Alzheimers Dis 2012;32(3):623–631.
3. Beaulieu C. The basis of anisotropic water diffusion in the nervous system: a technical review. NMR Biomed 2002;15(7-8):435–455.
4. O'Sullivan M, Jones DK, Summers PE, Morris RG, Williams SC, Markus HS. Evidence for cortical "disconnection" as a mechanism of age-related cognitive decline. Neurology 2001;57(4):632–638.
5. Oishi K, Mielke MM, Albert M, Lyketsos CG, Mori S. DTI analyses and clinical applications in Alzheimer's disease. J Alzheimers Dis 2011;26(Suppl 3):287–296.
6. Barrick TR, Charlton RA, Clark CA, Markus HS. White matter structural decline in normal ageing: a prospective longitudinal study using tract-based spatial statistics. Neuroimage 2010;51(2):565–577.
7. Teipel SJ, Meindl T, Wagner M, et al. Longitudinal changes in fiber tract integrity in healthy aging and mild cognitive impairment: a DTI follow-up study. J Alzheimers Dis 2010;22(2):507–522.
8. Sullivan EV, Rohlfing T, Pfefferbaum A. Longitudinal study of callosal microstructure in the normal adult aging brain using quantitative DTI fiber tracking. Dev Neuropsychol 2010;35(3):233–256.
9. Sexton CE, Walhovd KB, Storsve AB, et al. Accelerated changes in white matter microstructure during aging: a longitudinal diffusion tensor imaging study. J Neurosci 2014;34(46):15425–15436.
10. Vernooij MW, de Groot M, van der Lugt A, et al. White matter atrophy and lesion formation explain the loss of structural integrity of white matter in aging. Neuroimage 2008;43(3):470–477.
11. Abe O, Aoki S, Hayashi N, et al. Normal aging in the central nervous system: quantitative MR diffusion-tensor analysis. Neurobiol Aging 2002;23(3):433–441.
12. Burzynska AZ, Preuschhof C, Bäckman L, et al. Age-related differences in white matter microstructure: region-specific patterns of diffusivity. Neuroimage 2010;49(3):2104–2112.
13. Nusbaum AO, Tang CY, Buchsbaum MS, Wei TC, Atlas SW. Regional and global changes in cerebral diffusion with normal aging. AJNR Am J Neuroradiol 2001;22(1):136–142.
14. Lee DY, Fletcher E, Martinez O, et al. Vascular and degenerative processes differentially affect regional interhemispheric connections in normal aging, mild cognitive impairment, and Alzheimer disease. Stroke 2010;41(8):1791–1797.
15. de Groot M, Ikram MA, Akoudad S, et al. Tract-specific white matter degeneration in aging: the Rotterdam study. Alzheimers Dement 2015;11(3):321–330.
16. Hofman A, Darwish Murad S, van Duijn CM, et al. The Rotterdam study: 2014 objectives and design update. Eur J Epidemiol 2013;28(11):889–926.
17. Ikram MA, van der Lugt A, Niessen WJ, et al. The Rotterdam scan study: design and update up to 2012. Eur J Epidemiol 2011;26(10):811–824.
18. Vrooman HA, Cocosco CA, van der Lijn F, et al. Multi-spectral brain tissue segmentation using automatically trained k-Nearest-Neighbor classification. Neuroimage 2007;37(1):71–81.
19. de Boer R, Vrooman HA, van der Lijn F, et al. White matter lesion extension to automatic brain tissue segmentation on MRI. Neuroimage 2009;45(4):1151–1161.
20. Greve DN, Fischl B. Accurate and robust brain image alignment using boundary-based registration. Neuroimage 2009;48(1):63–72.
21. Koppelmans V, de Groot M, de Ruiter MB, et al. Global and focal white matter integrity in breast cancer survivors 20 years after adjuvant chemotherapy. Hum Brain Mapp 2014;35(3):889–899.
22. Leemans A, Jeurissen B, Sijbers J, Jones DK. ExploreDTI: a graphical toolbox for processing, analyzing, and visualizing diffusion MR data [abstr]. In: Proceedings of the Seventeenth Meeting of the International Society for Magnetic Resonance in Medicine. Berkeley, Calif: International Society for Magnetic Resonance in Medicine, 2009; 3537.
23. de Groot M, Vernooij MW, Klein S, et al. Improving alignment in tract-based spatial statistics: evaluation and optimization of image registration. Neuroimage 2013;76:400–411.

24. Smith SM, Jenkinson M, Johansen-Berg H, et al. Tract-based spatial statistics: voxelwise analysis of multi-subject diffusion data. Neuroimage 2006;31(4):1487–1505.

25. Jenkinson M, Beckmann CF, Behrens TE, Woolrich MW, Smith SM. FSL. Neuroimage 2012;62(2):782–790.

26. Smith SM, Nichols TE. Threshold-free cluster enhancement: addressing problems of smoothing, threshold dependence and localisation in cluster inference. Neuroimage 2009;44(1):83–98.

27. Nichols TE, Holmes AP. Nonparametric permutation tests for functional neuroimaging: a primer with examples. Hum Brain Mapp 2002;15(1):1–25.

28. Pierpaoli C, Barnett A, Pajevic S, et al. Water diffusion changes in Wallerian degeneration and their dependence on white matter architecture. Neuroimage 2001;13(6 Pt 1):1174–1185.

29. Douaud G, Jbabdi S, Behrens TE, et al. DTI measures in crossing-fibre areas: increased diffusion anisotropy reveals early white matter alteration in MCI and mild Alzheimer's disease. Neuroimage 2011;55(3):880–890.

30. Jeurissen B, Leemans A, Tournier JD, Jones DK, Sijbers J. Investigating the prevalence of complex fiber configurations in white matter tissue with diffusion magnetic resonance imaging. Hum Brain Mapp 2013;34(11):2747–2766.

31. Oishi K, Faria AV, van Zijl PCM, Mori S. MRI atlas of human white matter. 2nd ed. London, England: Academic Press, 2010.

32. Berlot R, Metzler-Baddeley C, Jones DK, O'Sullivan MJ. CSF contamination contributes to apparent microstructural alterations in mild cognitive impairment. Neuroimage 2014;92:27–35.

33. Persson J, Lind J, Larsson A, et al. Altered brain white matter integrity in healthy carriers of the APOE epsilon4 allele: a risk for AD? Neurology 2006;66(7):1029–1033.

34. Westlye LT, Reinvang I, Rootwelt H, Espeseth T. Effects of APOE on brain white matter microstructure in healthy adults. Neurology 2012;79(19):1961–1969.

35. Salat DH, Williams VJ, Leritz EC, et al. Inter-individual variation in blood pressure is associated with regional white matter integrity in generally healthy older adults. Neuroimage 2012;59(1):181–192.